Contribution from the Laboratoire de Chimie de Coordination du CNRS,
205 route de Narbonne, 31077 Toulouse Cedex, France

Olefin Epoxidation and Alkane Hydroxylation Catalyzed by Robust Sulfonated Manganese and Iron Porphyrins Supported on Cationic Ion-Exchange Resins

Sandro Campestrini and Bernard Meunier*

Received June 21, 1991

Robust sulfonated manganese and iron porphyrin supported on poly(vinylpyridinium) polymers have been used as catalysts in olefin epoxidation and alkane hydroxylation by iodosylbenzene. The metalloporphyrins are attached to protonated or methylated poly(vinylpyridine) polymers by the coordination of one pyridine unit, thus providing a proximal effect, and by additional interactions of the porphyrin sulfonato groups with the polymer pyridinium units. The best catalysts are the complexes containing halogen atoms at the pyrrole β-positions. In all these oxygenation reactions manganese porphyrins are better catalysts than the corresponding iron complexes. From comparative studies with another ion-exchange resin without a potential axial ligand, it can be noted that the concept of the proximal effect is a key factor in metalloporphyrin-catalyzed reactions, not only for soluble complexes but also for supported catalysts.

Introduction

After a decade on the modeling of cytochrome P-450 with soluble metalloporphyrin complexes associated with different oxygen atom donors[1,2] (iodosylbenzene, hypochlorite, organic or inorganic peroxides, molecular oxygen in the presence of a reducing agent), a new trend of this field is now to develop supported metalloporphyrin catalysts. The following advantages can be listed in favor of the use of supported catalysts: (i) a facile catalyst recovery, (ii) a physical separation of active sites by dispersion on the support and (iii) because of the large variety of possible supports, a modulation of the chemoselectivity, regioselectivity, and shape-selectivity of the oxygenation reactions catalyzed by these supported catalysts. Metalloporphyrins can be attached to polymers by covalent links,[3] but this approach implies a multistep synthesis of the porphyrin ligand or a chemical modification of the polymer, or only by a basic residue (imidazole or pyridine) acting as an axial ligand of the metalloporphyrin.[4] In this latter case, the fixation is reversible and usually both axial sites of iron–porphyrins are occupied, making impossible the formation of a transferrable iron–oxo species.

Another approach is to immobilize metalloporphyrins on (i) inorganic materials[5] (silica, alumina, zeolites[6] or clays) in order to have inert supports for catalytic oxidation reactions or (ii) on organic polymer-like ion-exchange resins.[7] We recently used sulfonated metalloporphyrins supported on cationic ion-exchange resins in the modeling of ligninase, a peroxidase involved in the oxidative degradation of lignin in wood.[8] These peroxidase models are also highly efficient in the oxidation of recalcitrant pollutants[9] like DDT or lindane, and they can be used to study the in vitro metabolism of drugs.[10] Two main advantages of these resin–metalloporphyrin catalysts can be listed: (i) they can be used in aqueous solutions, and (ii) because of a large number of available ion-exchange resins, it is possible to design highly sophisticated catalysts based on the understanding at the molecular level of interactions between the metalloporphyrin and the support. For example, in the case of poly(vinylpyridine) polymer, a "proximal effect" (i.e. the strong coordination of a basic ligand to the metalloporphyrin) is provided by some pyridine units of the polymer whereas the remaining residues, after protonation, are involved in the electrostatic interactions with sulfonato groups of the porphyrin ligand.[11]

Here we report the use of robust sulfonated iron and manganese porphyrins supported on poly(vinylpyridinium) polymers in olefin epoxidation and alkane hydroxylation reactions.[12] In the present study we used the sulfonated derivatives of *meso*-tetramesitylporphyrin (TMPS), *meso*-tetrakis(2,6-dichlorophenyl)porphyrin (TDCPPS), *meso*-tetramesityl-β-octabromoporphyrin (Br_8TMPS), and *meso*-tetrakis(3-chloro-2,4,6-trimethylphenyl)-β-octachloroporphyrin, Cl_{12}TMPSH_2.

The manganese and iron derivatives of the nonsulfonated ligand of these two latter porphyrins have been used as soluble catalysts

* To whom correspondence should be addressed.

(1) For review articles on metalloporphyrin-catalyzed reactions, see: (a) McMurry, T. J.; Groves, J. T. in *Cytochrome P-450: Structure, Mechanism and Biochemistry*; Ortiz de Montellano, P., Ed.; Plenum Press: New York, 1986; Chapter I. (b) Meunier, B. *Bull. Soc. Chim. Fr.* **1986**, 578–594. (c) Bruice, T. C. *Aldrichim. Acta* **1988**, *21*, 87–95. (d) Tabushi, I. *Coord. Chem. Rev.* **1988**, *86*, 1–42. (e) Montanari, F.; Banfi, S.; Quici, S. *Pure Appl. Chem.* **1989**, *61*, 1631–1636. (f) Khenkin, A. M.; Shilov, A. E. *New J. Chem.* **1989**, *13*, 659–667. (g) Mansuy, D. *Pure Appl. Chem.* **1990**, *62*, 741–746. (h) Meunier, B. *New J. Chem.* **1992**, *16*, 203–211.

(2) For some recent articles on metalloporphyrin-catalyzed oxidations, see: (a) Brown, R. B.; Hill, C. L. *J. Org. Chem.* **1988**, *53*, 5762–5768. (b) Robert, A.; Meunier, B. *New J. Chem.* **1988**, *12*, 885–896. (c) Tsuchiya, S.; Seno, M. *Chem. Lett.* **1989**, 263–266. (d) Groves, J. T.; Viski, P. *J. Am. Chem. Soc.* **1989**, *111*, 8537–8538. (e) Traylor, T. G.; Fann, W. P.; Bandyopadhyay, D. *Ibid.* **1989**, *111*, 8009–8010. (f) Haber, J.; Mlodnicka, T.; Poltowicz, J. *J. Mol. Catal.* **1989**, *54*, 451–461. (g) Collman, J. P.; Brauman, J. I.; Hampton, P. D.; Tanaka, H.; Scott Bohle, D.; Hembre, R. T. *J. Am. Chem. Soc.* **1990**, *112*, 7980–7984. (h) Nishihara, H.; Presspick, K.; Murray, R. W.; Collman, J. P. *Inorg. Chem.* **1990**, *29*, 1000–1006. (i) Hoffmann, P.; Labat, G.; Robert, A.; Meunier, B. *Tetrahedron Lett.* **1990**, *31*, 1991–1994. (j) Querci, C.; Ricci, M. *Ibid.* **1990**, *31*, 1779–1782. (k) Groves, J. T.; Ungashe, S. B. *J. Am. Chem. Soc.* **1990**, *112*, 7796–7797. (l) Banfi, S.; Maiocchi, A.; Moggi, A.; Montanari, F.; Quici, S. *J. Chem. Soc., Chem. Commun.* **1990**, 1794–1796. (m) Murata, K.; Panicucci, R.; Gopinath, E.; Bruice, T. C. *J. Am. Chem. Soc.* **1990**, *112*, 6072–6083. (n) Van der Made, A. W.; Nolte, R. J. M.; Drenth, W. *Recl. Trav. Chim. Pays-Bas* **1990**, *109*, 537–551. (o) Ellis, P. E.; Lyons, J. E. *Coord. Chem. Rev.* **1990**, *105*, 181–193. (p) Rodgers, K.; Arafa, I. M.; Goff, H. G. *J. Chem. Soc., Chem. Commun.* **1990**, 1323–1324. (q) Watanabe, Y.; Takehira, K.; Shimizu, M.; Hayakawa, T.; Orita, H. *J. Chem. Soc., Chem. Commun.* **1990**, 927–928. (r) Artaud, I.; Ben Aziza, K.; Chopard, C.; Mansuy, D. *Ibid.* **1991**, 31–33. (s) Robert, A.; Loock, B.; Momenteau, M.; Meunier, B. *Inorg. Chem.* **1991**, *30*, 706–711.

(3) (a) Leal, O.; Anderson, D. L.; Bowman, R. G.; Basolo, F.; Burwell, R. L. *J. Am. Chem. Soc.* **1975**, *97*, 5125–5129. (b) Tatsumi, T.; Nakamura, M.; Tominaga, H. *Chem. Lett.* **1989**, 419–420. (c) Rollmann, L. D. *Ibid.* **1975**, *97*, 2132–2136.

(4) Tsuchida, E.; Honda, K.; Hasegawa, E. *Biochem. Biophys. Acta* **1975**, *393*, 483–495 and references therein.

(5) (a) Fukuzumi, S.; Mochizuki, S.; Tanaka, T. *Isr. J. Chem.* **1987/88**, *28*, 29–36. (b) Kameyama, H.; Suzuki, H.; Amano, A. *Chem. Lett.* **1988**, 1117–1120. (c) Battioni, P.; Lalier, J. P.; Barloy, L.; Mansuy, D. *J. Chem. Soc., Chem. Commun.* **1989**, 1149–1151. (d) Barloy, L.; Battioni, P.; Mansuy, D. *Ibid.* **1990**, 1365–1367. (e) Nakamura, M.; Tatsumi, T.; Tominaga, H. *Bull. Chem. Soc. Jpn.* **1990**, *63*, 3334–3336.

(6) In the case of zeolite-encapsulated iron phthalocyanine or manganese Schiff base complexes, see: (a) Herron, N.; Stucky, G. D.; Tolman, C. A. *J. Chem. Soc., Chem. Commun.* **1986**, 1521–1522. (b) Herron, N. *J. Coord. Chem.* **1988**, *19*, 25–38. (c) Bowers, C.; Dutta, P. K. *J. Catal.* **1990**, *122*, 271–279.

(7) (a) Wöhrle, D.; Gitzel, J.; Krawczyk, G.; Tsuchida, E.; Ohno, H.; Okura, I.; Nishisaka, T. *J. Macromol. Sci. Chem.* **1988**, *A25*, 1227–1254. (b) Saito, Y.; Mifume, M.; Nakayama, H.; Odo, J.; Tanaka, Y.; Chikuma, M.; Tanaka, H. *Chem. Pharm. Bull.* **1987**, *35*, 869–872.

(8) (a) Labat, G.; Meunier, B. *J. Org. Chem.* **1989**, *54*, 5008–5011. (b) Labat, G.; Meunier, B. *New J. Chem.* **1989**, *13*, 801–804. (c) Labat, G.; Meunier, B. *Bull. Soc. Chim. Fr.* **1990**, *127*, 553–564.

0020-1669/92/1331-1999$03.00/0 © 1992 American Chemical Society

Chart I

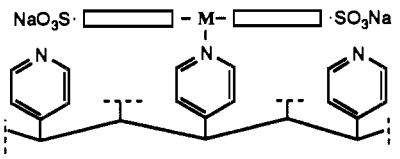

(M-Porph-S)-PVP

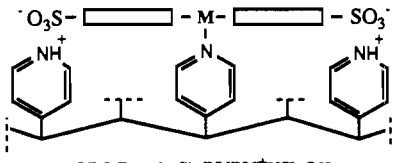

[(M-Porph-S)-PVPH$^+$][TsO$^-$]

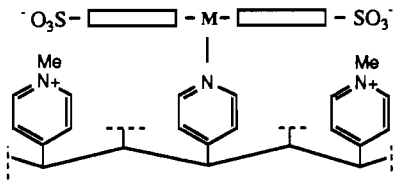

[(M-Porph-S)-PVPMe$^+$][TsO$^-$]

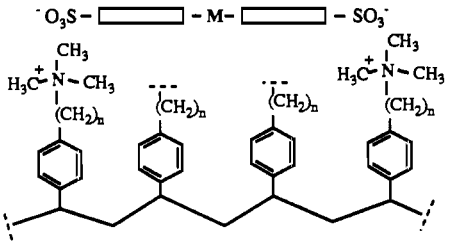

(M-Porph-S)-Amberlite-IRA-900

Chart II

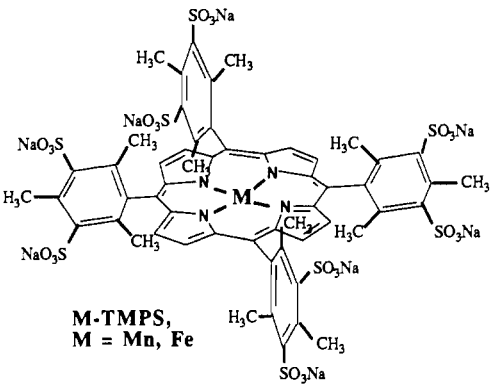

M-TMPS,
M = Mn, Fe

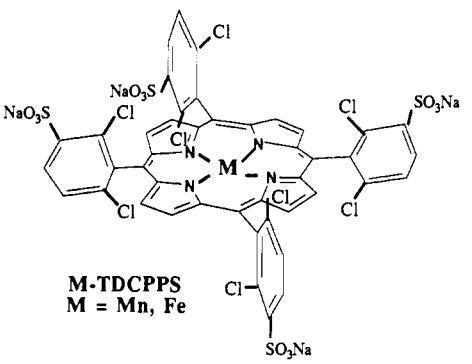

M-TDCPPS
M = Mn, Fe

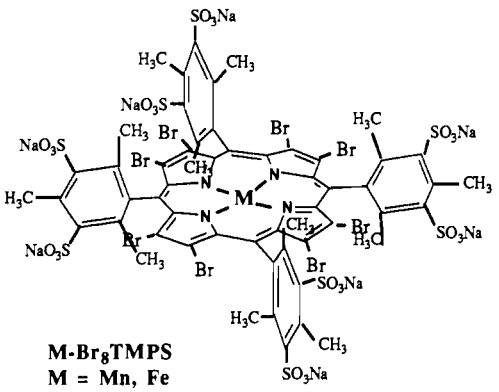

M-Br$_8$TMPS
M = Mn, Fe

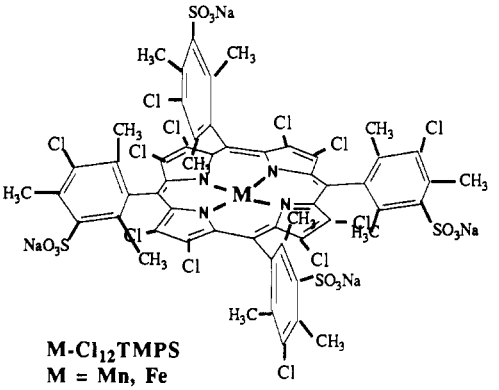

M-Cl$_{12}$TMPS
M = Mn, Fe

in oxygenation reactions performed in the liquid phase.[2i,13]

Results and Discussion

Preparation of Supported Metalloporphyrin on Poly(vinylpyridine) Polymers. The free poly(vinylpyridine) is obtained from an alkaline treatment of poly(4-vinylpyridinium–toluene-4-sulfonate) crosslinked with 2% divinylbenzene. This polymer contains 3.5 mmol of pyridine units/g of resin. Three different types of supported catalysts have been prepared: (i) by direct attachment of the manganese complex to the polymer by coordination of one pyridine unit to the complex, (ii) by further protonation of the remaining pyridine sites and creation of electrostatic interactions between polymer pyridiniums and the sulfonato groups of the metalloporphyrin, and (iii) by methylation of the free pyridine units (instead of protonation) (see Chart I). For the last two cases, [(M–Porp–S)–PVPH$^+$][TsO$^-$] and [(M–Porp–S)–PVPMe$^+$][TsO$^-$], there is an additional electrostatic interaction between the pyridinium units of the polymer and the sulfonato groups of the metalloporphyrin, assuring then a second strong binding of the catalyst to the support. These PVP polymers provide a proximal effect without addition of free pyridine in the reaction mixture. Different studies have shown that only one pyridine per manganese catalyst is sufficient to enhance the rate

(9) Labat, G.; Seris, J. L.; Meunier, B. *Angew. Chem., Int. Ed. Engl.* **1990**, *29*, 1471–1473.
(10) Bernadou, J.; Bonnafous, M.; Labat, G.; Loiseau, P.; Meunier, B. *Drug Metab. Disp.* **1991**, *19*, 360–365.
(11) Labat, G.; Meunier, B. *C. R. Acad. Sci. Paris* **1990**, *311* (II), 625–630.
(12) (a) During the accomplishment of the present study, the olefin epoxidation by PhIO catalyzed by iron porphyrins supported on ion-exchange resins was also reported: Leanord, D. R.; Lindsay Smith, J. R. *J. Chem. Soc., Perkin Trans 2*, **1990**, 1917–1923; **1991**, 25–30. (b) The use of a manganese porphyrin bound to colloidal anion-exchange particles in the NaOCl epoxidation of styrene appeared in the literature during the preparation of the present article: Turk, H.; Ford, W. T. *J. Org. Chem.* **1991**, *56*, 1253–1260.
(13) Hoffmann, P.; Robert, A.; Meunier, B. *Bull. Soc. Chim. Fr.*, in press.

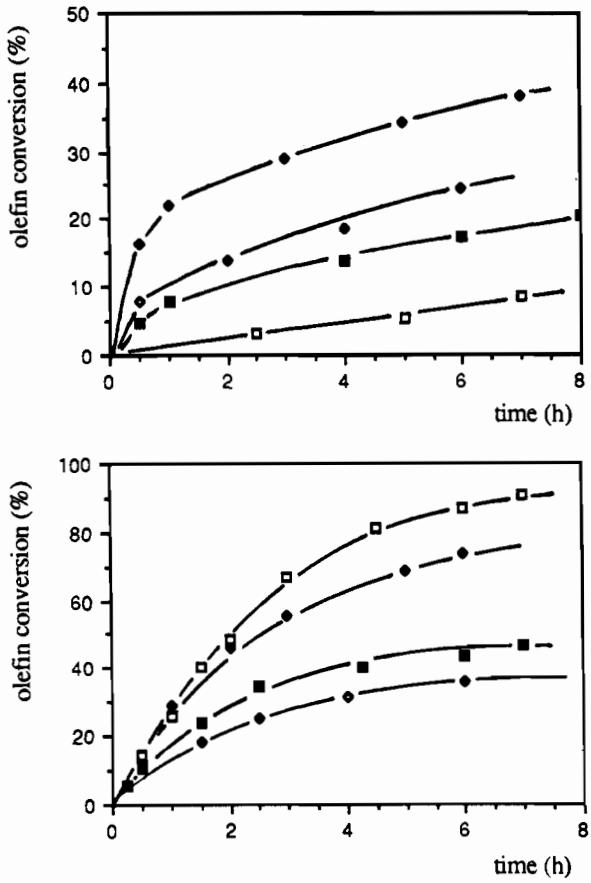

Figure 1. (a, Top) $[(n\text{-Bu})_4N]HSO_5$ oxidation of cyclooctene catalyzed by various sulfonated manganese porphyrins immobilized on methylated PVP, [Mn–porphyrin–S–PVPMe$^+$][TsO$^-$]: [MnTMPS–PVPMe$^+$][TsO$^-$] (◇); [$MnBr_8$TMPS–PVPMe$^+$][TsO$^-$] (◆); [MnTDCPPS–PVPMe$^+$][TsO$^-$] (■); without catalyst (□). Conditions: cyclooctene (150 μmol), $[(n\text{-Bu})_4N]HSO_5$ (240 μmol), Mn–porphyrin–S (2 μmol) immobilized on [PVPMe$^+$][TsO$^-$] (200 mg of PVP treated by TsOH or TsOMe) in 2 mL of dichloromethane at room temperature. (b, Bottom) PhIO oxidation of cyclooctene catalyzed by various sulfonated manganese porphyrin immobilized on methylated PVP, [Mn–porphyrin–S–PVPMe$^+$][TsO$^-$]: [MnTMPS–PVPMe$^+$][TsO$^-$] (◇); [$MnBr_8$TMPS–PVPMe$^+$][TsO$^-$] (◆); [MnTDCPPS–PVPMe$^+$][TsO$^-$] (■); [$MnCl_{12}$TMPS–PVPMe$^+$][TsO$^-$] (box). Conditions: cyclooctene (150 μmol), PhIO (750 μmol), Mn–porphyrin–S (2 μmol) immobilized on [PVPMe$^+$][TsO$^-$] (200 mg of PVP treated by TsOMe) in 3 mL of dichloromethane at room temperature.

of the catalytic oxygen atom transfer from the high-valent metal–oxo species to the organic substrate.[1b,e,2l,s,14] The advantages of PVP polymer over a cationic amberlite resin (see Chart I for structures) have been recently illustrated in the modeling of ligninase.[11] We used four different sulfonated porphyrin ligands. All of them are obtained by the oleum sulfonation of four robust porphyrins: *meso*-tetramesitylporphyrin ($TMPH_2$), *meso*-tetrakis(2,6-dichlorophenyl)porphyrin ($TDCPPH_2$), *meso*-tetramesityl-β-octabromoporphyrin (Br_8TMPH_2) and *meso*-tetrakis(3-chloro-2,4,6-trimethylphenyl)-β-octachloroporphyrin ($Cl_{12}TMPH_2$) (see Chart II for structures of used sulfonated metalloporphyrins).

Cyclooctene Epoxidation Catalyzed by Supported Sulfonated Metalloporphyrins. We first investigated the possible use of the tetra-*n*-butylammonium salt of monopersulfate, $[(n\text{-Bu})_4N]HSO_5$, since the potassium salt is only soluble in water and to avoid a ternary phase system, solid/liquid/liquid. Three manganese sulfonated porphyrins supported on methylated PVP have been used as catalysts: [MnTMPS–PVPMe$^+$][TsO$^-$], [MnTDCPPS–PVPMe$^+$][TsO$^-$], and [$MnBr_8$TMPS–PVPMe$^+$][TsO$^-$]. After 2 h of reaction at room temperature, the slope of the olefin conversion is the same as that of the noncatalyzed epoxidation (see Figure 1a), corresponding to the deactivation of the supported manganese porphyrins. The mechanism of this deactivation with the ammonium salt of monopersulfate is not clearly understood, since the soluble versions of these catalysts are robust, at least when monopersulfate is used in a biphasic solvent system. Even more, one related catalyst, Mn(Br_8TMP)Cl, is not destroyed by ozone in ozone metalloporphyrin-catalyzed epoxidation reactions.[15] One possible reason of the bleaching of these PVP-supported catalysts is an extraction of the sulfonated metalloporphyrin from the polymer surface by the lipophilic ammonium salt followed by the catalyst bleaching due to the excess of $[(n\text{-Bu})_4N]HSO_5$ in the organic phase.

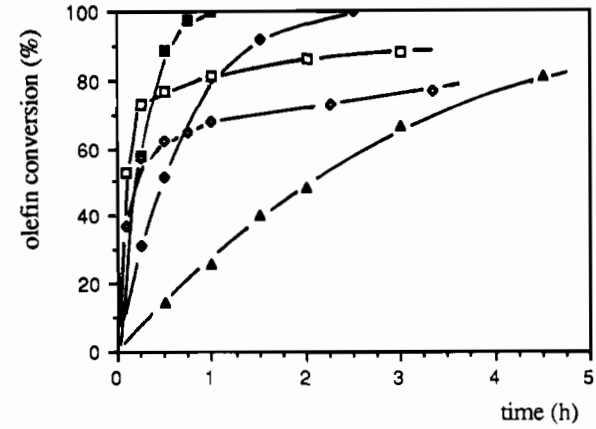

Figure 2. PhIO oxidation of cyclooctene catalyzed by $[MnCl_{12}TMPS][(n\text{-Bu})_4N]_4$ in the presence (box) or in the absence (◇) of pyridine and the same complex immobilized on different forms of poly(vinylpyridine) polymers: [$MnCl_{12}$TMPS–PVP] (◆); [$MnCl_{12}$TMPS–PVPH$^+$][TsO$^-$] (▲); [$MnCl_{12}$TMPS–PVPMe$^+$][TsO$^-$] (■). Conditions: cyclooctene (150 μmol), PhIO (750 μmol), $[MnCl_{12}TMPS][(n\text{-Bu})_4N]_4$ (2 μmol without or with 100 μmol of pyridine) or $MnCl_{12}$TMPS (2 μmol) immobilized on PVP (200 mg) or cationic PVP (200 mg of PVP treated by TsOH or TsOMe) in 3 mL of dichloromethane at room temperature.

So we decided to investigate the behavior of PhIO as oxygen donor with these catalysts supported on PVP. The results of the PhIO epoxidation of cyclooctene catalyzed by [MnTMPS–PVPMe$^+$][TsO$^-$], [MnTDCPPS–PVPMe$^+$][TsO$^-$], [$MnBr_8$TMPS–PVPMe$^+$][TsO$^-$], and [$MnCl_{12}$TMPS–PVPMe$^+$][TsO$^-$] are reported in Figure 1b. No epoxide formation is detected when PhIO is used with PVP or methylated PVP (PhIO is not decomposed by these polymers). But for a low loading of methylated PVP by the four sulfonated manganese porphyrin complexes and a catalyst/substrate molar ratio equal to 1.3%, an efficient catalytic epoxidation of cyclooctene is observed: 90% of the olefin is converted by [$MnCl_{12}$TMPS–PVPMe$^+$][TsO$^-$] in 7 h at room temperature (the turnover rate of this reaction is 18 cycles/h, based on the first 50% of olefin conversion). The two best catalysts are halogenated on the pyrrolic β-positions, the less active being the PVP-supported MnTDCPPS, just below the activity of the analogue catalyst based on tetramesitylporphyrin. When PhIO/CH_2Cl_2 is replaced by H_2O_2/CH_3CN, no reaction occurs.

The activity of these PVP-supported catalysts were compared to a soluble form of the most active sulfonated manganese derivative, the tetra-*n*-butylammonium salt of $MnCl_{12}$TMPS. The soluble catalyst, $[MnCl_{12}TMPS][(n\text{-Bu})_4N]_4$, has nearly the same activity as [$MnCl_{12}$TMPS–PVP] in the PhIO epoxidation of cyclooctene (Figure 2). But in the presence of pyridine (50 equiv versus catalyst), $[MnCl_{12}TMPS][(n\text{-Bu})_4N]_4$ has the same initial activity as [$MnCl_{12}$TMPS–PVPMe$^+$][TsO$^-$]. However, the olefin conversion slows down after 75–80%, whereas cyclooctene is

(14) (a) Guilmet, E.; Meunier, B. *Nouv. J. Chim.* **1982**, *6*, 511–513. (b) Meunier, B.; de Carvalho, M. E.; Bortolini, O.; Momenteau, M. *Inorg. Chem.* **1988**, *27*, 161–164. (c) Banfi, S.; Montanari, F.; Quici, S. *J. Org. Chem.* **1989**, *54*, 1850–1859.

(15) Campestrini, S.; Robert, A.; Meunier, B. *J. Org. Chem.* **1991**, *56*, 3725–3727.

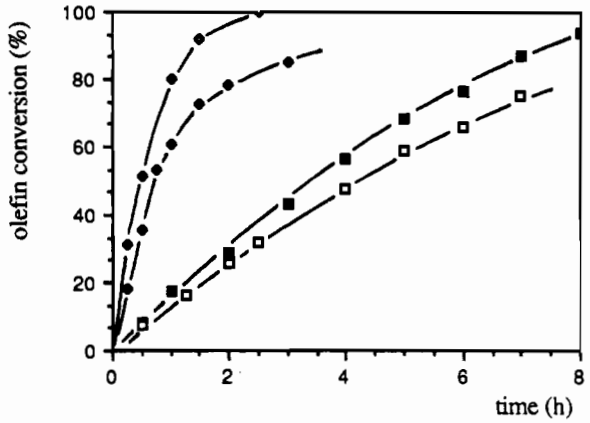

Figure 3. PhIO oxidation of cyclooctene catalyzed by $MnCl_{12}TMPS$ immobilized on PVP (diamond) or amberlite-IRA-900 (squares), in the absence (empty symbols) or in the presence of pyridine (full symbols). Conditions: cyclooctene (150 μmol), PhIO (750 μmol), $MnCl_{12}TMPS$ (2 μmol) immobilized on PVP (200 mg) or Amberlite-IRA-900 without or with pyridine (100 μmol) in 3 mL of dichloromethane at room temperature.

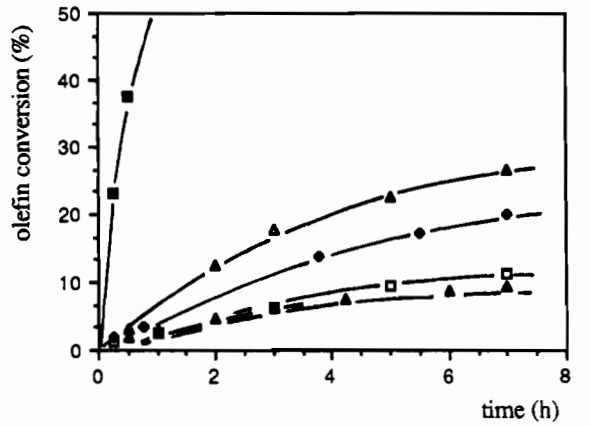

Figure 4. PhIO oxidation of cyclooctene catalyzed by $MnBr_8TMPS$ (■) or $FeBr_8TMPS$ (▲) immobilized on PVP, by MnTMPS immobilized on Amberlite-IRA-900, in the presence (100 μmol, ▲) or in the absence (□) of pyridine and FeTMPS immobilized on the same polymer (♦). Conditions: cyclooctene (150 μmol), PhIO (750 μmol), MBr_8TMPS (2 μmol) immobilized on PVP (200 mg) or MTMPS (2 μmol) immobilized on Amberlite-IRA-900 (200 mg) in 3 mL of dichloromethane at room temperature.

completely oxidized in the case of the supported catalyst. This suggests that the supported catalyst is protected from partial destruction or from inhibition. For larger quantities of olefin this inflection point is not observed for the soluble manganese catalyst, suggesting then that this loss of activity at high conversion is probably due to a inhibition reaction rather than a partial destruction of the catalyst.

When these supported sulfonated manganese complexes are immobilized on a cationic ion-exchange resin without a proximal ligand arising from the polymer, i.e. in the case of amberlite-IRA-900 (see Chart I for structures of supported catalysts on this type of resin), the addition of free pyridine has small effect on the increase of olefin conversion (see Figure 3). This effect is less pronounced than for soluble catalysts[1b,e,14] and might result from two opposite effects. The coordination of pyridine has to occur mainly on the porphyrin face which is opposite to the polymer and consequently obliges the active metal–oxo to be generated within a cavity, close to the polymer. This situation will contribute to the inhibition of the reaction. But an oxo–manganese porphyrin with an axial pyridine is more active than an oxo–manganese species without pyridine. The balance of these two opposite factors might explain the small effect of pyridine. More remarkable is the negative effect of pyridine on the same catalyst supported on methylated PVP (Figure 3). In this case, one axial ligand is already occupied by a pyridine arising from PVP, so the presence of free pyridine leads to the formation of a bis(pyridine) adduct (one pyridine from PVP and the second one from the added free pyridine) which is inactive in catalysis. Previous studies have effectively indicated that the best ligand/manganese ratio for a strong proximal effect in oxygenation reactions catalyzed by manganese porphyrins is 1.[14]

Supported iron porphyrins are less reactive than the corresponding manganese derivatives in the PhIO epoxidation of cyclooctene (Figure 4). Olefin conversion (80%) was reached with [$MnBr_8TMPS$–PVP] in 2 h, whereas only 10% was obtained with [$FeBr_8TMPS$–PVP] in 6 h. When immobilized on amberlite, FeTMPS also had a poor activity, 20% of olefin conversion in 7 h, slightly above that of MnTMPS–amberlite without addition of free pyridine, but below that of the same immobilized manganese catalyst in the presence of free pyridine (50 equiv versus catalyst). Manganese porphyrins are always more active than the corresponding iron complexes in catalytic epoxidations. The same behavior is also observed for immobilized metalloporphyrin on cationic ion-exchange resins.

Recycling Experiments with $MnCl_{12}TMPS$ Immobilized on Methylated PVP. Figure 5a describes the formation of cyclootene oxide when the same $MnCl_{12}TMPS$ catalyst supported on methylated PVP is recycled four times, while Figure 5b reports the conversion of PhIO for the same four reactions. A noticeable

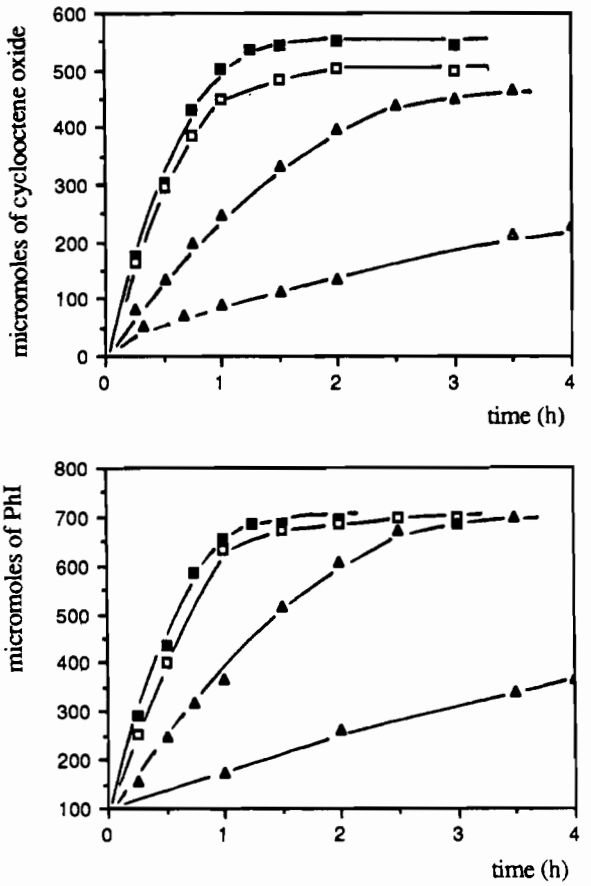

Figure 5. Epoxide yield (a, top) and PhI formation (b, bottom) in the PhIO epoxidation of cyclooctene catalyzed by $MnCl_{12}TMPS$ immobilized on [$PVPMe^+$][TsO^-]. The curves represent four consecutive experiments by recycling the same supported catalyst: (■) first run; (□) second run; (▲) third run; (△) fourth run. Conditions: cyclooctene (3840 μmol), PhIO (750 μmol), $MnCl_{12}TMPS$ (1 μmol) immobilized on [$PVPMe^+$][TsO^-] (100 mg of PVP treated by TsOMe) in 3 mL of dichloromethane at room temperature.

loss of activity is observed in both cases for the fourth cycle. For [$MnCl_{12}TMPS$–$PVPMe^+$][TsO^-], it should be noted that the two first cycles are exactly the same; a small activity decrease is observed for the third run (Figure 5b). With 1 μmol of $MnCl_{12}TMPS$ immobilized on [$PVPMe^+$][TsO^-] the total epoxide production after four runs is 1970 μmol (and 2175 μmol after five runs). The overall selectivity versus PhIO is 65%. These ex-

Table I. Cyclooctene Oxidation by PhIO Catalyzed by Recycled $[MnCl_{12}TMPS][n\text{-}Bu)_4N]_4$[a]

run	time, min	yield of cyclooctene oxide, μmol	total amt of cyclooctene oxide, μmol
1	30	105	105
2	30	125	230
3	30	125	355
4	45	134	489
5	30	126	615
6	30	115	730
7	35	156	886
8	45	109	965
9	90	105	1100

[a] Experimental conditions: for the first run cyclooctene (150 μmol), PhIO (170 μmol), $[MnCl_{12}TMPS][(n\text{-}Bu)_4N]_4$ (2 μmol), and pyridine (100 μmol) have been added to 3 mL of CH_2Cl_2 under magnetic stirring at room temperature. Runs from 2 to 9 have been performed by adding to the initial reaction mixture 150 μmol of cyclooctene and 170 μmol of PhIO each time.

Table II. Cyclooctene Oxidation by PhIO Catalyzed by Recycled $[MnCl_{12}TMPS][(n\text{-}Bu)_4]_4$[a]

run	time, min	yield of cyclooctene oxide, μmol	total yield of cyclooctene oxide, μmol
1	60	518	518
2	60	532	1050
3	45	485	1535
4	75	508	2043
5	75	490	2533
6	105	463	2996

[a] Experimental conditions: for the first run cyclooctene (7500 μmol), PhIO (750 μmol), $[MnCl_{12}TMPS][(n\text{-}Bu)_4N]_4$ (2 μmol), and pyridine (100 μmol) have been added to 3 mL of CH_2Cl_2 under magnetic stirring at room temperature. Runs from 2 to 6 have been performed by adding to the initial reaction mixture 750 μmol of PhIO each time.

periments were run with a large excess of oxidant and olefin with respect to the supported catalyst. We checked the stability of the soluble form of this supported catalyst, $[MnCl_{12}TMPS][(n\text{-}Bu)_4N]_4$ in the epoxidation of cyclooctene by PhIO. Nine runs were performed with the same initial catalyst (2 μmol) using 150 μmol of olefin and 170 μmol of PhIO for each cycle (see results in Table I). The average catalytic activity for the first eight runs was 1.8 cycles/min. In these conditions 550 mol of epoxide were obtained per mole of catalyst. The overall "epoxide/converted PhIO" selectivity was 72%. Such a higher selectivity value found for the homogeneous epoxidation reaction, compared to the supported reaction, indicates that the catalytic decomposition of PhIO is more important on the supported catalyst.

A better catalytic activity was obtained when the oxidant was added by fractions (Table II), starting with 7500 μmol of olefin for 2 μmol of $[MnCl_{12}TMPS][(n\text{-}Bu)_4N]_4$ and 750 μmol of PhIO for each run. The average catalytic activity during the first five runs was 4.2 cycles/min, and the total amount of produce epoxide was 2996 μmol, i.e. nearly 1500 epoxide molecules per catalyst molecule. In these conditions, the epoxide/converted PhIO selectivity was 67%.

$MnCl_{12}TMPS$ being one of the most efficient catalyst for the olefin epoxidation, we decided to investigate its activity, after immobilization on PVP polymers, in the hydroxylation of saturated hydrocarbons.

Adamantane Hydroxylation by PhIO Catalyzed by $MnCl_{12}TMPS$ Supported on PVP Polymers. First of all, the different forms of PVP-supported $MnCl_{12}TMPS$ were compared to the same manganese porphyrin immobilized on amberlite-IRA-900 (Table III). The distribution of adamantane derivatives was analyzed after 2 and 7 h of reaction at room temperature. $[MnCl_{12}TMPS–PVPMe^+][TsO^-]$ gave the highest selectivity ratio for adamantanols versus adamantanone (53), indicating that the hydroxylation reaction is actually the main oxidation reaction with this catalyst. With the same catalyst, the product distribution did not change after 2 h at room temperature, 312 μmol of adamantanols and adamantanone were produced within 2 h compared to 322 μmol in 7 h. Amberlite is not suitable compared to methylated PVP (or even PVP) as a support. Only 50 μmol of adamantanols and adamantanone were formed by $MnCl_{12}TMPS$–amberlite in 7 h compared to 322 μmol with the same catalyst on methylated PVP.

When the same batch of $[MnCl_{12}TMPS–PVPMe^+][TsO^-]$ catalyst, which has been used for the experiments detailed in Table III, is used after being stored for 2 months in a flask under air, nearly the same catalytic activity is obtained in the hydroxylation of adamantane. The catalyst aspect changed: the fine powder turned to a gum (uptake of moisture). However, in the same experimental conditions of Table III, the total yield of adamantane derivatives (ols + one) based on PhIO was 32%, the total turnover number was 240, the ols/one ratio was 57, and the C_{tert}/C_{sec} ratio was 3.4 (after statistical correction, 4 tertiary C–H bonds/12 secondary C–H bonds). These data compare well with those obtained with the fresh catalyst: 43%, 322, 53, and 3.2, respectively. One of the most striking of these PhIO oxidations of adamantane catalyzed by $MnCl_{12}TMPS$ supported on methylated PVP is the low C_{tert}/C_{sec} ratio, 3.2–4.2. This low value is an intrinsic property of $MnCl_{12}TMPS$ itself, since we found the same low values for the soluble form of this catalyst (see below). With other soluble iron porphyrin catalysts associated to PhIO, the C_{tert}/C_{sec} selectivity is high (11–48) and agrees with the abstraction of a hydrogen atom from the substrate by a nonsterically hindered active iron–oxo species.[16] With potassium monopersulfate and Mn(TDCPP)Cl as catalyst, we observed a C_{tert}/C_{sec} ratio of 10.[2b] High shape selectivities have been observed in alkane hydroxylation by Suslick et al. using highly hindered metalloporphyrin catalysts, but no data are available on the C_{tert}/C_{sec} ratio in the adamantane oxidation with these hindered complexes.[17] The PhIO oxidation of adamantane by the soluble $[MnCl_{12}TMPS][(n\text{-}Bu)_4N]_4$ catalyst was performed in dichloromethane (Table IV). The homogeneous reaction is slower than with the supported catalyst. The total yield of oxidized adamantane derivatives versus PhIO is 54% after 96 h. After these 4 days, corresponding to the complete consumption of PhIO, the catalyst was not destroyed. Before the addition of PhIO, the solution is green (Soret band at 494 nm) and turned to red-orange after the oxidant addition (Soret band at 456 nm). When all PhIO is consumed, the solution changed back to green and the Soret was observed again at 494 nm without apparent loss of intensity. The ols/one ratio is 18, and the C_{tert}/C_{sec} ratio is 4.2. This value is slightly higher than that obtained with the immobilized catalyst forms, suggesting that the selectivity for secondary C–H bond hydroxylation is enhanced by interactions between the porphyrin complex and the support.

PhIO Oxidation of *n*-Octane Catalyzed by $MnCl_{12}TMPS$ Supported on PVP Polymers. Since the reactivity ratio C_{tert}/C_{sec} was low in the oxidation of adamantane catalyzed by soluble or immobilized $MnCl_{12}TMPS$, suggesting a high shape selectivity, it was tempting to investigate alcohol and ketone distribution in the hydroxylation of an aliphatic alkane like *n*-octane. The PhIO oxidation of *n*-octane was performed with the soluble form of $MnCl_{12}TMPS$, $[MnCl_{12}TMPS][(n\text{-}Bu)_4N]_4$, and two immobilized forms of the same catalyst, $[MnCl_{12}TMPS–PVP]$ and $[MnCl_{12}TMPS–PVPMe^+][TsO^-]$ (see results in Table V). As expected, reactions are slower with *n*-octane than with adamantane since there are no tertiary C–H bonds available in this *n*-alkane. Up to 124 turnovers were observed in 120 h at room temperature. At this point, the ols/ones ratio was 1.9 and the amount of 1-octanol was low, the reactivity ratio C_{sec}/C_{prim} being 44 (3 tertiary C–H bonds for 3 × 2 secondary C–H bonds). The immobilization of $MnCl_{12}TMPS$ on PVP alone was not sufficient to improve the catalytic oxidation. A better activity was obtained with $[MnCl_{12}TMPS–PVPMe^+][TsO^-]$, at least for the first hours of the reaction. The octane conversion was 76 turnovers within 7

(16) Groves, J. T.; Nemo, T. E. *J. Am. Chem. Soc.* **1983**, *105*, 6243–6248.
(17) Cook, B. R.; Reinert, T. J.; Suslick, K. S. *J. Am. Chem. Soc.* **1986**, *108*, 7281–7286.

Table III. Oxidation of Adamantane by PhIO Catalyzed by $MnCl_{12}TMPS$ Immobilized on Different Supports[a]

support	yield of products, μmol (after 7 h)				ols/one ratio	yield/PhIO, %
	Ad-1-ol	Ad-2-ol	Ad-2-one	total		
PVP	145	82	11	238	21	33[e]
$[PVPH^+][TsO^-]$	131	60	8	199	24	28
$[PVPMe^+][TsO^-]$	166 (159)[d]	150 (147)	6 (6)	322 (312)	53 (51)	44 (43)
$[PVPMe^+][TsO^-]$[b]	120 (120)	64 (64)	6 (6)	190 (190)	31 (31)	26 (26)
amberlite-IRA-900	30	17	3	50	16	7
amberlite-IRA-900[c]	28	12	3	43	13	6

[a] Conditions: adamantane (3860 μmol), PhIO (750 μmol), $MnCl_{12}TMPS$ (1 μmol) immobilized on 100 mg of PVP or 250 mg of protonated (or methylated) PVP, or on 250 mg of amberlite-IRA-900, in 7 mL of CH_2Cl_2 under magnetic stirring, at room temperature. [b] *m*-$ClPhCO_3H$ was used as oxidant (750 μmol). [c] Run in the presence of pyridine (100 μmol). [d] Data after only 2 h at room temperature. [e] These data correspond to the molar ratio (Ad-1-ol + Ad-2-ol + 2Ad-2-one)/PhIO.

Table IV. Oxidation of Adamantane by PhIO Catalyzed by $[MnCl_{12}TMPS][(n\text{-}Bu)_4N]_4$ in the Presence of Pyridine[a]

reaction time, h	yield of products, μmol				ols/one ratio	yield/PhIO,[b] %
	Ad-1-ol	Ad-2-ol	Ad-2-ol	total		
1	28	18	0	36		6
2	43	31	0	74		10
4	53	40	0	93		13
7	64	45	5	114	22	16
24	131	85	12	232	18	32
96	226	142	20	388	18	55

[a] Conditions: adamantane (3860 μmol), PhIO (750 μmol), $[MnCl_{12}TMPS][(n\text{-}Bu)_4N]_4$ (1 μmol), pyridine (50 μmol) in 7 mL of CH_2Cl_2 under magnetic stirring, at room temperature. [b] These data correspond to the molar ratio (Ad-1-ol + Ad-2-ol + 2Ad-2-one)/PhIO.

Table V. Oxidation of *n*-Octane by PhIO Catalyzed by $MnCl_{12}TMPS$ Immobilized on Different Supports[a]

support	yield of products, μmol					
	alcohols[b]		1-octanol		ketones[c]	
	7 h	24 h	7 h	24 h	7 h	24 h
no[d]	20	27	0	0	9	15
PVP	13	17[e]	0	0	4	7[f]
$[PVPMe^+][TsO^-]$	70	70[g]	2	2	6	6[h]

[a] Conditions: *n*-octane (4000 μmol), PhIO (750 μmol), $[MnCl_{12}TMPS][(n\text{-}Bu)_4N]_4$ (1 μmol) or $MnCl_{12}TMPS$ (1 μmol) immobilzed on 100 mg of PVP or 250 mg of methylated PVP in 7 mL of CH_2Cl_2 under magnetic stirring, at room temperature. [b] Addition of 2-octanol, 3-octanol, and 4-octanol yields. [c] Addition of 2-octanone, 3-octanone, and 4-octanone yields. [d] $[MnCl_{12}TMPS][(n\text{-}Bu)_4N]_4$ as catalyst. [e] 2-Octanol/3-octanol/4-octanol ratio = 40/30/30%. [f] 2-Octanone/3-octanone/4-octanone ratio = 40/33/27%. [g] 1-Octanol/2-octanol/3-octanol/4-octanol ratio = 2/37/30/31%. [h] 2-Octanone/3-octanone/4-octanone ratio = 40/30/30%.

h. The selectivity for alcohols was also improved, the ols/ones ratio and the reactivity ratio C_{sec}/C_{prim} being 11 and 21, respectively (compared to 1.9 and 44 for the soluble catalyst). The immobilization of the sulfonated manganese porphyrin has a noticeable influence on the selectivity of the oxidation. However, the ratio 1-octanol/secondary octanols (i.e. ω-hydroxylation versus ω-1, ω-2, and ω-3 hydroxylations) remained below that one observed with the best known soluble manganese porphyrin catalyst for the ω-hydroxylation, [*meso*-tetrakis(2,4,6-triphenylphenyl)-porphyrinato]manganese.[17] With this latter complex up to 26% of the total amount of alcohols corresponded to the hydroxylation of the terminal methyl, compared to 2% in the present case.

PhIO is a competitive substrate with the olefin or the alkane in the oxygenation reactions. The catalytic overoxidation of PhIO to iodoxybenzene,[18] $PhIO_2$, was studied with the three type of supported manganese catalyst, $[MnCl_{12}TMPS\text{–}PVP]$, $[MnCl_{12}TMPS\text{–}PVPH^+][TsO^-]$, and $[MnCl_{12}TMPS\text{–}PVPMe^+][TsO^-]$ (see results in Table VI). PhIO (62, 50, and 58%; 465, 375, and 435 μmol) was converted within 2 h by

(18) Nappa, M. J.; Tolman, C. A. *Inorg. Chem.* **1985**, *24*, 4711–4719.

Table VI. Decomposition of PhIO Catalyzed by $MnCl_{12}TMPS$ Immobilized on Different Supports[a]

time, h	PhIO conversion, μmol[b]		
	PVP	$[PVPH^+]$-$[TsO^-]$	$[PVPMe^+]$-$[TsO^-]$
0.25	105,[c] 210[d] (36)[e]	180, 345 (17)	233, 270 (72)
0.5	150, 382 (63)	255, 375 (27)	278, 450 (113)
1	270, 645 (96)	300, 450 (42)	353, 570 (119)
2	465, 675 (101)	375, 465 (68)	435, 630 (119)
4	615	428, 540 (101)	548

[a] Conditions: PhIO (750 μmol), $MnCl_{12}TMPS$ (2 μmol) immobilized on 100 mg of PVP or 250 mg of protonated (or methylated) PVP in 3 mL of CH_2Cl_2 at room temperature. [b] PhIO conversion was calculated by PhI determination. In the absence of $MnCl_{12}TMPS$ no decomposition of PhIO occurred. [c] Number of micromoles of converted PhIO in the absence of olefin. [d] Number of micromoles of converted PhIO in the presence of 150 μmol of cyclooctene. [e] The number of micromoles of formed cyclooctene oxide are indicated in parentheses.

Chart III

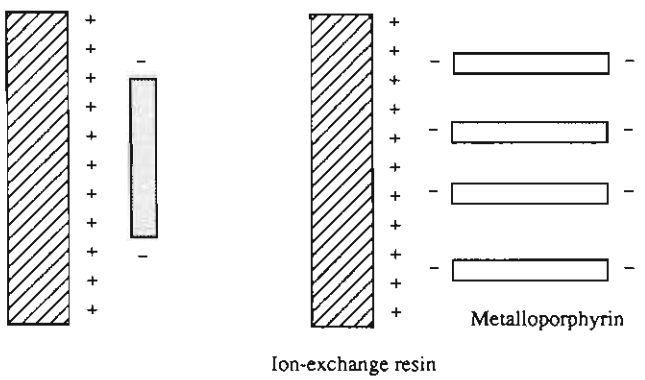

Coating Mode (A) **Stacking Mode (B)**

$[MnCl_{12}TMPS\text{–}PVP]$, $[MnCl_{12}TMPS\text{–}PVPH^+][TsO^-]$, and $[MnCl_{12}TMPS\text{–}PVPMe^+][TsO^-]$, respectively. In the presence of cyclooctene, the PhIO conversions were 90, 62, and 84% (675, 465, and 630 μmol), respectively. In all cases the overoxidation of PhIO to $PhIO_2$ was not reduced by the presence of the olefin since the quantity of converted PhIO was always slightly above the quantity of PhIO converted in the absence of cyclooctene. These data confirmed that the PhIO oxidation by the reactive high-valent metal–oxo species is not inhibited by an olefin.

Final Remarks and Conclusion

The main features of these PhIO oxygenation reactions catalyzed by manganese and iron porphyrins supported on cationic ion-exchange resins are the following.

(i) The poly(vinylpyridinium) resins lead to catalysts better than other simple cationic resins, because of the proximal effect due to the coordination of a pyridine unit arising from the polymer. In addition to the known favorable role of the proximal pyridine on the different steps of the metalloporphyrin activation (rate enhancement of both metal–oxo formation and oxygen atom

transfer steps), the double interaction of sulfonated metalloporphyrin with poly(vinylpyridinium) polymers (pyridine proximal effect and sulfonato–pyridinium interactions) immobilized the catalyst more strictly on the support than the simple electrostatic interactions on amberlite type resins. In the latter case, there is probably an equilibrium between two possible types of interactions: the "coating" mode (A in Chart III) and the "stacking" mode (B in Chart III). In mode B, the stacking of metalloporphyrins enhances the bleaching of the supported catalyst when the high-valent metal–oxo species are formed. This phenomenon was observed by Lindsay Smith in the case of a cationic iron porphyrin catalyst supported on anionic polymers[12a] and by our group for cationic manganese porphyrins in interactions with DNA (a naturally-occurring anionic polymer).[19]

(ii) These poly(vinylpyridinium)-supported catalysts have efficiencies similar to those of the corresponding metalloporphyrin complexes in solution, even with PhIO which is not highly soluble in dichloromethane. The reaction is actually a triphasic system: solid/solid/liquid (polymeric PhIO/supported catalyst/olefin in dichloromethane).

(iii) The most efficient supported metallorporphyrin catalysts for oxygenation reactions are those with manganese as the central metal and with halogen atoms at the pyrrole β-positions.

(iv) The best PVP–manganese catalysts can be recycled three or four times, and up to 2175 cycles can be achieved in the epoxidation of cyclooctene before a significant loss of catalytic activity.

In conclusion, *the concept of the proximal effect is a key factor in metalloporphyrin-catalyzed reactions, not only for soluble complexes but also for supported catalysts.* We are currently extending the use of these poly(vinylpyridinium)–manganese porphyrin catalysts for other oxidation reactions.

Experimental Section

Materials and Chemicals. Gas chromatographic analyses were performed as previously described.[2b] UV–visible spectra were recorded on a Cary 2300 spectrophotometer. Chemicals were purchased from Aldrich or Janssen. Peroxides were removed from olefins by passing them through a short column of Florisil before use. Potassium monopersulfate (a triple salt, $2KHSO_5$, $KHSO_4$, K_2SO_4) was a gift from Degussa (Caroat) or from Interox (Curox). Iodosylbenzene was prepared from iodobenzene diacetate.[20] Dichloromethane (99.95%) was used without purification. The porphyrin ligands $TMPH_2$, $TDCPPH_2$ and Br_8TMPH_2 were prepared using a modified Lindsey method.[13,21] *meso*-Tetramesityl-β-octabromoporphyrin, Br_8TMPH_2, was obtained by NBS bromination of the pyrrole β-positions of $TMPH_2$.[2i,13] *meso*-Tetrakis(3-chloro-2,4,6-trimethylphenyl)-β-octachloroporphyrin, $Cl_{12}TMPH_2$, is the major product of tetramesitylporphyrin with *N*-chlorosuccinimide.[13]

Sulfonation of $TMPH_2$, $TDCPPH_2$ and Br_8TMPH_2 was performed with an oleum solution (H_2SO_4 with 18–24% of SO_3, Aldrich) according to Srivastava and Tsutsui.[22,23] Metalation of these ligands by $Mn(OAc)_2$ was conducted in refluxing DMF, in the presence of 10 equiv of 2,4,6-collidine, for 4–6 h. The preparation of the latter porphyrin, $Cl_{12}TMPSH_2$, was performed as described below.

***meso*-Tetrakis(3-chloro-5-sulfonato-2,4,6-trimethylphenyl)-β-octachloroporphyrin, Sodium Salt ($Cl_{12}TMPSH_2$).** A 300-mg sample of $Cl_{12}TMPH_2$ (251 μmol) was stirred at 80 °C for 30 min in 3 mL of an 18–24% oleum solution. To the cold reaction mixture was slowly added 10 mL of water. This solution was neutralized with a concentrated NaOH solution (4.5 g in 30 mL of water). In fact, at the end of the NaOH addition the pH was 8–9. Sodium sulfate was removed by precipitation upon addition of methanol at 0 °C. The resulting solution was concentrated and treated again by methanol at 0 °C three times. After evaporation, the solid residue was dissolved in a minimum of methanol and the resulting solution was filtered; the filtrate gave 340 mg of crude $Cl_{12}TMPS$. In water, the Soret band is observed at 458 nm. The proton NMR spectrum confirms that the sulfonation site was the last meta C–H of the mesityl groups (the sulfonation level is always above 3.7–3.9 sulfonato groups per porphyrin ligand) ($C_{56}H_{38}N_4Cl_{12}Na_4O_{12}S_4$, MW = 1605).

Manganese Complex of $Cl_{12}TMPSH_2$ ($MnCl_{12}TMPS$). A 450-mg (280 μmol) sample of $Cl_{12}TMPS$, 10 equiv of $Mn(OAc)_2$ (700 mg), and 1 mL of 2,4,6-collidine (20 equiv) were refluxed in 100 mL of DMF for 4 h (metalation was complete). After evaporation under pump vacuum, the green solid material was dissolved in 90 mL of methanol and the resulting solution was filtered. The filtrate was evaporated, and the residue was dissolved in water, treated on a column packed with a cationic ion-exchange resin, Biorad AG 50W-X8 (hydrogen form, 200–400 mesh), and washed with water. After elution with water, the manganese porphyrin solution was neutralized by NaOH (4 M) up to pH 8. The solution was evaporated, the solid was dissolved in 5 mL of methanol, and the resulting solution was filtrated. This solution was chromatographed on Sephadex LH20 with methanol as eluent (yield = 90%). Because of the NaOH treatment the axial ligand was probably an hydroxo group ($C_{56}H_{37}N_4Cl_{12}Na_4MnO_{13}S_4$, MW = 1675). The Soret band is observed at 487 nm (water), and the two α and β bands were observed at 595 and 630 nm (the ratio of the absorbances at 487 and 595 is 8.0; since the complex is highly hygroscopic and is contaminated by salts, ε values are fluctuating).

Preparation of $[MnCl_{12}TMPS][(n\text{-}Bu)_4N]_4$. A 50-mg (29 μmol) sample of $MnCl_{12}TMPS$ and 400 mg of $(n\text{-}Bu)_4NHSO_4$ were dissolved in 20 mL of water. The manganese porphyrin derivative was extracted with 60 mL of dichloromethane. After evaporation, the solid residue is washed three times with water and dried under vacuum. The yield is quantitative ($C_{120}H_{181}N_8Cl_{12}MnO_{13}S_4$, MW = 2552, with a hydroxo group as the axial ligand). Three characteristic UV–visible bands are observed in dichloromethane: 492 (Soret), 595, and 630 nm (absorbance ratio at 492/595 = 10.3).

Preparation of Supported Manganese Porphyrin Complexes on Poly(vinylpyridine) Polymers (PVP). First, free poly(vinylpyridine) was obtained by treating 3.0 g of poly(4-vinylpyridinium–toluene-4-sulfonate) cross-linked with 2% of divinylbenzene (Fluka, 3.5 mmol of toluene-4-sulfonate/g of resin) with a 0.5 M solution of NaOH for 30 min. After filtration, the polymer was washed with water until neutral pH and then with acetone and finally dried under vacuum. A total of 1.2 g of PVP was recovered (1.0 g of this reticulated PVP corresponds to 8.5 mmol of pyridine sites). $[MnCl_{12}TMPS–PVP]$ corresponds to the direct attachment of the manganese complex to the polymer by coordination of one pyridine unit to the complex, $[MnCl_{12}TMPS–PVPH^+][TsO^-]$ corresponds to the protonation of the remaining pyridine sites of the previous supported catalyst (creation of electrostatic interactions between polymer pyridiniums and the sulfonato groups of the metalloporphyrin), and $[MnCl_{12}TMPS–PVPMe^+][TsO^-]$ corresponds to the methylation of the free pyridine units (instead of protonation). Such preparations are described for $MnCl_{12}TMPS$ and are available for any other sulfonated metalloporphyrin complexes.

$[MnCl_{12}TMPS–PVP]$. A 1.0-g sample of PVP (see above) was added to a solution of 16.5 mg of $MnCl_{12}TMPS$ (10 μmol) in 50 mL of methanol. The solution became nearly colorless after an overnight gentle magnetic stirring. After evaporation, the solid residue was washed with 20 mL of water and 100 mL of acetone and dried under vacuum. No metalloporphyrin was released during the washing steps. The loading corresponds to 1 over 850 pyridines used as the proximal ligand and 550 ppm of manganese on the polymer.

$[MnCl_{12}TMPS–PVPH^+][TsO^-]$. $[MnCl_{12}TMPS–PVP]$ (200 mg), prepared as indicated above, was stirred for 30 min in an aqueous solution of *p*-toluenesulfonic acid (0.4 g of TsOH in 30 mL of water). After filtration, the polymer was washed with 100 mL of acetone and dried under vacuum. A total of 500 mg of $[MnCl_{12}TMPS–PVPH^+][TsO^-]$ was recovered (quantitative yield).

$[MnCl_{12}TMPS–PVPMe^+][TsO^-]$. $[MnCl_{12}TMPS–PVP]$ (1.0 g) was treated with a solution of methyl *p*-toluenesulfonate in DMF (16 g of TsOMe in 50 mL of DMF) for 2 h at 60 °C and 48 h at room temperature under a gentle stirring. After filtration, the polymer was washed with 50 mL of dichloromethane and 100 mL of acetone and finally dried under vacuum. A total of 2.5 g of $[MnCl_{12}TMPS–PVPMe^+][TsO^-]$ was recovered (yield = 95%).

UV–Visible Spectra of Supported Sulfonated Manganese Porphyrins on Poly(vinylpyridinium) Polymers. The UV–visible spectra recorded on a spectrophotometer equipped with an integration sphere gave poor quality spectra, whereas spectra obtained from Vaseline mull gave rather well-defined spectra (see Figure 6 for the UV–visible spectrum of $[MnCl_{12}TMPS–PVPMe^+][TsO^-]$). The supported manganese porphyrin on the poly(vinylpyridinium) polymer was crushed in Vaseline in order to obtain a mull. This colored mull was deposited on the external face of a 2-mm-thick UV–vis cuvette and the spectrum recorded as usual. The baseline was high and had to be corrected. The Soret band is blue-shifted

(19) Ding, L.; Bernadou, J.; Meunier, B. *Bioconjugate Chem.* **1991**, *2*, 201–206.
(20) Saltzman, H.; Sharefkin, J. G. *Org. Synth.* **1963**, *43*, 60–61.
(21) Lindsey, J. S.; Wagner, R. W. *J. Org. Chem.* **1989**, *54*, 828–836.
(22) Srivastava, T. S.; Tsutsui, M. J. *J. Org. Chem.* **1973**, *38*, 2103.
(23) Labat, G. Thèse de l'Université Paul Sabatier, Dec. 1989. For other recent reports on preparation of TDCPPS, see refs 12 and 24.
(24) Dolphin, D. H.; Nakano, T.; Kirk, T. K.; Maione, T. E.; Farrell, R. L.; Wijesekera, T. P. Patent PCT Int. Appl. WO 88/07988, 1988.

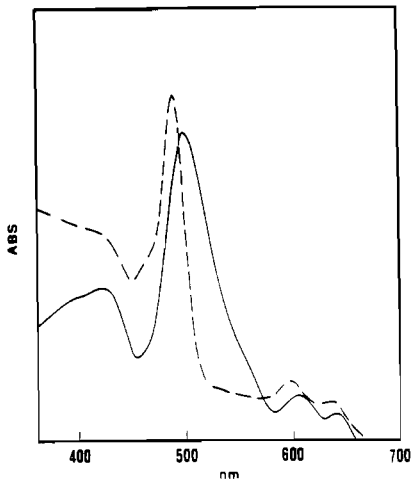

Figure 6. UV-visible spectra of $MnCl_{12}TMPS$ (full lines) and $[MnCl_{12}TMPS-PVPMe^+][TsO^-]$ (dotted lines) in Vaseline.

(from 497 to 490 nm) as expected for the coordination of a nitrogen-containing ligand to a manganese porphyrin.[25]

Preparation of $[(n\text{-Bu})_4N]HSO_5$. Tetra-*n*-butylammonium monopersulfate was prepared from the potassium salt using the procedure published by Trost et al. with some modifications.[26] A 2.0-g sample of potassium monopersulfate (6.5 mmol) in 20 mL of water was stirred with 2.0 g of tetra-*n*-butylammonium hydrogen sulfate (5.9 mmol) for 20 min. Then the solution was extracted with 40 mL of dichloromethane. This organic phase was dried over magnesium sulfate and filtered out. After evaporation, the remaining paste was washed with 10 mL of hexane and dried under vacuum. After evaporation, 0.5 g of $[(n\text{-Bu})_4N]HSO_5$ was obtained with a purity better than 90% (determined by iodometric titration). ***Caution***: this peroxide should be considered as potentially explosive, and despite the repeated number of safe syntheses, we never overpassed this preparation scale.

Typical Procedure for Cyclooctene Epoxidations Catalyzed by Supported Manganese Porphyrin Complexes. A 5-mL flask was loaded with 3 mL of dichloromethane, 20 μL of cyclooctene (154 μmol), 20 μL of 1,2-dichlorobenzene (178 μmol) as internal standard for GC analyses, and 2 μmol of sulfonated manganese porphyrin loaded on 100 mg of PVP (or 2 μmol of sulfonated manganese porphyrin for ~250 mg of loaded and protonated or methylated PVP resin). At time zero, 165 mg of PhIO (750 μmol) was added to the stirred reaction mixture. At different reaction times the stirring was stopped to allow the uptake of an aliquot of 1 μL, which was directly analyzed by GC. Concentrations of cyclooctene and cyclooctene oxide were determined after their corresponding response factors. Results described in Figure 5 were obtained starting with 500 μL of cyclooctene (3850 μmol).

Typical Procedure for Adamantane Hydroxylations Catalyzed by Supported Manganese Porphyrin Complexes. A 10-mL flask was loaded with 525 mg of adamantane (3.86 mmol), 120 mg of 1,4-dibromobenzene (internal standard), 1 μmol of the supported catalyst, and 7 mL of dichloromethane (1 μmol of the supported catalyst equals a loading of 1 μmol of $MnCl_{12}TMPS$ for 100 mg of PVP in the case of $[MnCl_{12}TMPS-PVP]$, or for ~250 mg of $[MnCl_{12}TMPS-PVPH^+][TsO^-]$ or $[MnCl_{12}TMPS-PVPMe^+][TsO^-]$). At time zero, 165 mg of PhIO (750 μmmol) was added to the stirred reaction mixture at room temperature under air (results were not modified when performed in an argon atmosphere). Aliquots of 1 μL were directly analyzed by GC. Concentrations of 1-admantanol, 2-adamantanol, and adamantanone were determined after their corresponding response factors.

Acknowledgment. This work was supported by a "Stimulation" grant from the EEC, including a postdoctoral fellowship for S.C. (on leave from Prs. G. Modena and F. Di Furia laboratory, Padova University). Dr. Anne Robert is gratefully acknowledged for fruitful discussions throughout this work and interpretations of NMR spectra. We are indebted to two referees for detailed remarks and comments.

(25) Kelly, S. L.; Kadish, K. M. *Inorg. Chem.* **1982**, *21*, 3631-3639.
(26) Trost, B. M.; Braslau, R. *J. Org. Chem.* **1988**, *53*, 532-537.

Contribution from the Department of Chemistry, United States Naval Academy, Annapolis, Maryland 21402, Department of Chemistry and Biochemistry, University of Delaware, Newark, Delaware 19716, and Department of Chemistry, The Catholic University of America, Washington, D.C. 20064

Iron Octaethyltetraazaporphyrins: Synthesis, Characterization, Coordination Chemistry, and Comparisons to Related Iron Porphyrins and Phthalocyanines

Jeffrey P. Fitzgerald,*,† Brian S. Haggerty,‡ Arnold L. Rheingold,‡ Leopold May,§ and Gregory A. Brewer§

Received January 31, 1992

This paper describes the synthesis and characterization of a series of iron octaethyltetraazaporphyrin complexes and a comparison of these substances to related iron porphyrins and phthalocyanines. Experimental evidence provided by magnetic susceptibility measurements, ^1H NMR, EPR, and Mössbauer spectroscopies, cyclic voltammetry, and/or X-ray crystallography indicates the tetraazaporphyrin ligand is a stronger σ donor and π acceptor than is a porphyrin ligand. Due to its high σ basicity, the tetraazaporphyrin ligand stabilizes the unusual $S = {}^3/_2$ spin state for iron in chloroiron(III) octaethyltetraazaporphyrin. Yet the high π acidity of the tetraazaporphyrin ligand shifts iron III/II redox potentials 400 mV positive of those for analogous iron porphyrins. In this sense, the tetraazaporphyrin macrocycle is more like a phthalocyanine than a porphyrin. Compared to phthalocyanines, octaethyltetraazaporphyrins are readily soluble. The high solubility, unusual metal spin states, and positively shifted redox potentials of octaethyltetraazaporphyrins suggest that they may have better or unique catalytic properties than porphryins or phthalocyanines.

Tetraazaporphyrins (**1**), also known as porphyrazines, are a class of aromatic, macrocyclic ligands composed of four pyrrole rings bridged by aza nitrogen atoms. These molecules may be considered to be structural hybrids of the well-studied porphyrins (**2**) (four pyrrole rings connected by methine carbon atoms) and phthalocyanines (**3**) (four isoindole rings bridged by aza nitrogen atoms). As such, tetraazaporphyrins provide an excellent opportunity to explore the subtle effects of ligand structure on the properties of coordinated metal ions in porphyrinic complexes.

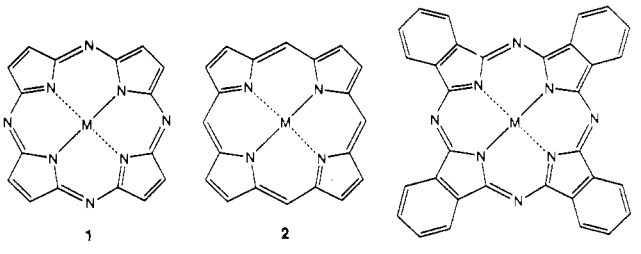

† United States Naval Academy.
‡ Universty of Delaware.
§ The Catholic University of America.

0020-1669/92/1331-2006$03.00/0 © 1992 American Chemical Society